Modern Physics Letters B, Vol. 20, No. 9 (2006) 451–474

World Scientific
www.worldscientific.com

INVESTIGATION ON THE MICROSCOPIC STRUCTURE OF E'_δ CENTER IN AMORPHOUS SILICON DIOXIDE BY ELECTRON PARAMAGNETIC RESONANCE SPECTROSCOPY

G. BUSCARINO*, S. AGNELLO and F. M. GELARDI

Department of Physical and Astronomical Sciences,
University of Palermo, Palermo, Via Archirafi 36, I-90123, Italy
**buscarin@fisica.unipa.it*

Received 26 January 2006

The E'_δ center is one of the most important paramagnetic point defects in amorphous silicon dioxide (a-SiO_2) primarily for applications in the field of electronics. In fact, its appearance in the gate oxide of metal-oxide-semiconductor (MOS) structures seriously affects the proper work of many devices and, often, causes their definitive failure. In spite of its relevance, until now a definitive microscopic model of this point defect has not been established. In the present work we review our experimental investigation by electron paramagnetic resonance (EPR) on the E'_δ center induced in γ-ray irradiated a-SiO_2. This study has driven us to the determination of the intensity ratio between the hyperfine doublet and the main resonance line of this point defect. On the basis of this estimation we have pointed out that the unpaired electron wave function of the E'_δ center is actually delocalized over four nearly equivalent silicon atoms, shedding new light on the microscopic structure of this technologically relevant point defect.

Keywords: Amorphous silicon dioxide; point defect; E' centers.

1. Introduction

Amorphous silicon dioxide (a-SiO_2) is a key materials in many of the modern technologies in the fields of optics and electronics.[1,2] The main reason of interest on this material is due to the fact that a-SiO_2 is found as a gate in almost the totality of the modern metal-oxide-semiconductor (MOS) devices.[1–4] Exposition of these systems to ionizing radiation causes the growth of several types of point defects in a-SiO_2, affecting the proper work of the devices and, in many cases, causing their definitive failure.[1–4] Point defects influence the electronics properties of MOS devices by trapping charges in the oxide, whose principal effect is to induce a deleterious threshold voltage shift.[4] Since 1950 many experimental investigations have been done to characterize the defects responsible for the charge trapping in a-SiO_2, primarily carried out by electron paramagnetic resonance (EPR) spectroscopy. These studies have pointed out that the electronic properties of MOS devices are prevalently affected by two paramagnetic point defects in a-SiO_2: E'_γ and E'_δ centers.[1–7]

The E'_γ center is characterized by an almost axially symmetric EPR line shape with a zero crossing spectroscopic splitting factor g value of ~ 2.0006. This defect has been widely studied and its most accepted model consists in a puckered positively charged oxygen vacancy: O≡Si* O≡Si$^+$ (where ≡ represents the bonds to three oxygen atoms, * represents an unpaired electron and $^+$ is a trapped hole).[8–10] In this model it is supposed that, following ionization of the vacancy, the positively charged Si atom moves backward through the plane of its basal oxygens in a puckered configuration.[10] As a consequence of this structural relaxation, the unpaired electron localizes in an sp^3 hybrid orbital of the unpuckered Si atom.[1,2,9,10] This structural model followed the definitive attribution to the same defect of a doublet of EPR lines split by ~ 42 mT, arising from the hyperfine interaction of the unpaired electron with a ^{29}Si nucleus (4.7% natural abundant isotope with nuclear spin $I = 1/2$).[8,9] Following the above reported microscopic model, the E'_γ center is considered as the equivalent in a-SiO_2 of the E'_1 center of α-quartz,[1,2,11–16] the most common crystalline form of SiO_2. Recently, the existence of another type of E'_γ center consisting only in the O≡Si* moiety, i.e. without the positively charged counterpart, has been also proposed.[17]

The E'_δ center is characterized by a highly symmetric EPR line shape with zero crossing g value of ~ 2.002 and a pair of lines split by ~ 10 mT, supposed to arise from the hyperfine interaction of the unpaired electron with a ^{29}Si nucleus.[18] The E'_δ point defect has been observed in bulk a-SiO_2,[18–24] in thermally grown a-SiO_2 films on Si,[25–37] and in buried oxide layer of separation by implantation of oxygen (SIMOX) systems.[25,32,38–46] These experimental works have pointed out that the E'_δ center can be induced in a-SiO_2 by X- and γ-ray irradiation, hole injection and by bombardment with Ar^+ ions. Although all these treatments are able to induce the E'_δ center, large differences in the generation efficiency have been found. Bombardment with Ar^+ ions, for example, was found to be at least tree orders of magnitude more efficient in generating E'_δ center with respect to hole injection and X- or γ-ray irradiation.[45] Furthermore, it has been pointed out that holes injection is able to induce E'_δ centers in many a-SiO_2 on Si systems, whereas an equal number of injected electrons does not.[27,28,42] This experimental evidence has been considered as an indication of the hole trapped nature of the E'_δ center.[27,28,42]

A key experimental evidence on E'_δ center consists in the observation that a large number of its precursors are induced during high temperature ($T > 1000$°C) annealing in different atmospheres of buried[26,32,33,35] and unburied[32,34–37] a-SiO_2 films on Si. In the same works a similar generation process has been also observed for the precursors of the E'_γ center. To explain these findings, it has been proposed that during thermal treatments O atoms could diffuse from the a-SiO_2 layer to the substrate and to the polysilicon overlayer, the driving force of this process being the different solubility limit of O in Si and SiO_2.[26,33,47] In this scheme, the generation of precursors of E'_γ and E'_δ centers in the a-SiO_2 layer should be due to the out-diffusion of oxygen from the oxide and the formation of oxygen vacancies.[26,33,47]

Nevertheless, the observation of SiO gas production during low pressure oxidation of silicon,[48] has inspired a different model in which is supposed that during high temperature treatments the freeing of volatile SiO at the Si/SiO_2 interface, through the reduction reaction $Si + SiO_2 \rightarrow 2\ SiO$ (volatile), could occur.[32,34,36,37,48] In this case, oxygen deficient defects could be induced by the rearrangement within the oxide network of volatile SiO, freed from the interface and diffusing through the oxide.[37] Although the exact process responsible for the thermally induced degradation of MOS structures is not fully clarified, its occurrence clearly indicates the intrinsic and oxygen deficiency related nature of the E'_δ center.

An intriguing feature regarding the E'_δ center is that in the same materials in which this center is induced, another characteristic EPR signal with $g \sim 4$ is also found.[18–20,22–24] This resonance has been attributed to a weakly allowed transition between the states $|m_s = -1\rangle$ and $|m_s = +1\rangle$ of a coupled spins system in a triplet state ($S = 1$).[18,49] As a consequence of the observation of a similar growth of concentration with increasing X-ray irradiation dose it has been suggested that the triplet center could share the same precursor of E'_δ center.[20] In this scheme, a single and a double ionization of the same precursor site could originate the E'_δ and the triplet center, respectively.[18,19,20,22–24]

The microscopic structure of the E'_δ center is still not univocally determined. Since its first observation, many distinct microscopic models have been proposed. Griscom and Friebele observed that:[18]

(i) the ^{29}Si hyperfine splitting of the E'_δ center (~ 10 mT) is ~ 4 times smaller than that of the E'_γ center (~ 42 mT),
(ii) the g tensor of E'_δ center is nearly isotropic.

These features were explained supposing that the unpaired electron of the E'_δ center is delocalized over four symmetrically disposed Si sp^3 orbitals similar to the one involved in the E'_γ center.[18] Furthermore, since the concentration of E'_δ center was found to correlate with the Cl content of the materials, a model consisting in an electron delocalized over four Si sp^3 orbitals of an $[SiO_4]^{4+}$ vacancy decorated by three Cl^- ions was proposed (4-Si Cl-containing model).[18] However, as the same authors pointed out, the absence of the EPR lines due to the hyperfine interaction of the unpaired electron with the $I = 3/2$ nuclei of ^{35}Cl and ^{37}Cl (with 75.4% and 24.6% natural abundance, respectively) represented a serious difficulty for the reliability of this model. The possibility that F atoms, together with Cl, could be involved in the microscopic structure of the E'_δ center has also been raised by Tohmon *et al.*[19] However, in successive works it has been reported that the E'_δ defect can be equivalently induced in Cl- and F-free samples, ruling out definitively the direct involvement of these impurities in the E'_δ center.[27,28,43,44]

Tohmon *et al.*[19] have pointed out that a necessary condition for the formation of the E'_δ center is the oxygen deficiency of the material, estimated by measuring the intensity of the absorption band peaked at ~ 5.0 eV. Furthermore, the authors have shown that as a consequence of a thermal treatment at 500°C in atmosphere

of H_2, the 5.0 eV band is destroyed together with the precursors of the E'_δ centers.[19] On the basis of these observations a microscopic model was proposed for the E'_δ center consisting in an ionized single oxygen vacancy with the unpaired electron nearly equally shared by the two Si atoms (2-Si model).[19]

Vanheusden and Stesmans[43,44] have reported that E'_γ and E'_δ are induced in SIMOX samples. Furthermore, the authors have shown that E'_δ centers are prevalently induced in the region 200 Å ÷ 700 Å away from the BOX/substrate interface, whereas E'_γ centers are localized in a more extended region in the BOX. Since it was known that a large number of Si inclusions occur in the same region of the BOX in which the E'_δ centers are induced,[50,51] a new microscopic model was proposed in which the unpaired electron of the defect was supposed to be delocalized over the four sp^3 hybrid orbitals of a silicon atom disposed at the center of a five Si cluster (5-Si model).[43,44] Successively, the authors have verified the occurrence of Si inclusions in their samples by Transmission Electron Microscopy (TEM) and Atomic Force Microscopy (AFM) and have proposed a model to explain the processes responsible of their retention in the BOX structures.[52–55]

Zhang and Leisure[20] have focused on the experimental estimation of the EPR intensity ratio, ζ, between the 10 mT doublet and the E'_δ main line. However, due to the low concentration of defects, the authors[20] have detected the 10 mT doublet in the high-power second-harmonic mode (SH-EPR), which allows high sensitivity. This scheme of acquisition cannot give quantitative information on the number of defects responsible for the EPR signal and consequently the ratio ζ cannot be determined. Nevertheless, *postulating* a strict similarity between the properties of E'_γ and E'_δ centers' SH-EPR signals, the authors could estimate $\zeta \cong 0.175$, indicating a delocalization of the unpaired electron over four equivalent Si atoms.[20] On the basis of this estimation, it has been proposed a microscopic model for the E'_δ center consisting in an $[SiO_4]^+$ vacancy, comprising four Si neighboring atoms, with the unpaired electron delocalized over the four sp^3 hybrid orbitals of the silicon atoms pointing towards the vacancy (4-Si model).[20]

Conley and Lenahan[46] have studied the effects on E'_γ and E'_δ centers of a room temperature treatment in hydrogen atmosphere (10% H_2 + 90% N_2). The authors have found that, as a consequence of the interaction with H_2, the EPR intensity of the E'_γ center decreases in concomitance with the growth of a doublet split by 7.4 mT. Similarly, the EPR intensity of the E'_δ center decreased with a simultaneous growth of a doublet split by $\sim$7.8 mT. Furthermore, both these conversion processes were found to take place in few minutes and saturate within two hours. The two doublets split by 7.4 mT and 7.8 mT were associated to hydrogen complexed E'_γ [56] and E'_δ centers, respectively. The authors,[46] on the basis of the similarity in the doublets splitting and in the time scales of the processes of interaction with H_2, have proposed that the E'_δ center could posses a microscopic structure similar to that of E'_γ center, with the unpaired electron strongly localized on a single Si atom (1-Si model).

The atomic and electronic structure of the E'_δ center has been explored in many simulative calculations using Density Functional Theory (DFT),[57–61] Hartree-Fock (HF),[62–66] and Embedded Cluster[67–70] methods. Chavez *et al.*[62] and Karna *et al.*[63] have studied the electronic structure of 2-Si, 4-Si and 5-Si models of the E'_δ center, and have shown that in all the cases considered the unpaired spin preferentially localizes on a single pair of Si atoms, so supporting the 2-Si model. However, in these calculations the atoms of the clusters were not allowed to relax after ionization. Consequently if, as suggested,[18,20,43,44] the delocalization of the unpaired electron results from a structural relaxation following the ionization of the precursor, then the conclusions outlined in these works could be questioned. Successive works focused on the electronic properties of the ionized single oxygen vacancy (2-Si model).[57–61,64–70] These works have pointed out that the ionized single oxygen vacancy in a-SiO_2, at variance of quartz, could admit a stable configuration in which the unpaired electron is nearly equally shared by the two Si atoms (2-Si model). This structure differs from that of E'_γ because the puckering does not occur. To test if the 2-Si model could actually represent a realistic model for the E'_δ center, the hyperfine structure[57,59,62,63,68–70] and the principal g values[69,70] have been predicted. The hyperfine structure has been found to consist of a doublet of lines split by 8 mT–13.5 mT, in good agreement with the experimental observations.[18–20,22,24] At variance, the calculated principal g values differ significantly from those obtained by EPR spectroscopy.[18,27,28,33,42–45] Furthermore, the calculated g values for the 2-Si model point out that this structure has a very low symmetry, whereas the EPR spectrum of the E'_δ center indicates an almost spherical symmetric unpaired electron wave function.[18]

2. Electron Paramagnetic Resonance Spectroscopy

In a typical EPR spectrometer the paramagnetic sample is placed in a static and uniform magnetic field $\mathbf{H}$. The effect of this field on the system under study is described by the Zeeman Hamiltonian operator:[49,71]

$$\mathcal{H}_{\text{zeeman}} = -\boldsymbol{\mu} \cdot \mathbf{H} \tag{1}$$

where $\boldsymbol{\mu}$ is the magnetic moment of the paramagnetic centers. In the simple and common case in which the magnetic moments are due to the electronic spin angular moments, the Zeeman Hamiltonian can be simplified as follow:

$$\mathcal{H}_{\text{zeeman}} = g_e \mu_{\text{B}} \mathbf{S} \cdot \mathbf{H} \tag{2}$$

where $g_e \cong 2.00232$ is the electronic splitting factor, $\mu_{\text{B}} = 9.27408 \cdot 10^{-24}$ J/T is the Bohr magnetic moment and $\mathbf{S}$ is the spin operator in units of $\hbar = h/2\pi = (1/2\pi) \cdot 6.62618 \cdot 10^{-34}$ J/s. The eigenvalues of $\mathcal{H}_{\text{zeeman}}$, which represent the energy levels of the system, are given by

$$\varepsilon_m = g_e \mu_{\text{B}} H m \tag{3}$$

where m is the eigenvalue of the component of $\mathbf{S}$ along the direction of $\mathbf{H}$. Equation (3) shows that, as a consequence of the interaction of the paramagnetic system with the static magnetic field (Zeeman interaction), a splitting of the energy levels with different m values occurs. In EPR experiments the system is contemporarily subjected to a second magnetic field $\mathbf{H}_1$ directed perpendicularly to $\mathbf{H}$ and with amplitude oscillating at a microwave frequency.[49,71,72] The aim of this oscillating field is to induce transitions between pairs of states energetically separated by the Zeeman interaction. These transitions occur when the quantum energy of the microwave photons, $h\nu$, matches the energy difference between a pair of levels with $m = j$ and $m = j+1$, where the magnetic dipole selection rules $\Delta m = \pm 1$ have been imposed.[49,71,72] The acquisition of an EPR spectrum consists in the measurement of the energy absorbed by the paramagnetic system as a function of the amplitude of $\mathbf{H}$ and at fixed amplitude and frequency of the magnetic field $\mathbf{H}_1$.[49,71,72]

2.1. *Systems with spin $S = 1/2$*

2.1.1. *Spectroscopic splitting tensor $\hat{g}$*

For systems in which the magnetic moment μ is due to the electron spin $S = 1/2$, which are of principal interest in the present work, the energies of the states with $m = 1/2$ and $m = -1/2$ are simply

$$\varepsilon_{\pm 1/2} = \pm \frac{1}{2} g_e \mu_{\mathrm{B}} H \tag{4}$$

and the resonance occurs when

$$h\nu = g_e \mu_{\mathrm{B}} H \tag{5}$$

where ν is the frequency of the oscillating magnetic field $\mathbf{H}_1$. Note that from Eq. (5) it follows that for a simple system of paramagnetic centers with $S = 1/2$ only a transition in correspondence to a static magnetic field $H_r = h\nu/g_e\mu_{\mathrm{B}}$ occurs.

Until now we have supposed that the paramagnetic centers are isolated. However, in many physical systems of interest, as for many point defects in solids, the paramagnetic centers interact with the surrounding atoms and consequently the EPR spectrum differs significantly with respect to that described by the Hamiltonian of Eq. (2). One of the most important consequences of these interactions is that, due to the spin-orbit interaction between the electron spin and orbital angular moments, the electronic spectroscopic splitting factor g_e has to be replaced by a matrix operator.[49,71] Consequently, the Zeeman interaction has to be described by the following Hamiltonian:[49,71,73]

$$\mathcal{H}_{\mathrm{zeeman}} = \mu_{\mathrm{B}} \mathbf{S} \cdot \hat{\mathbf{g}} \cdot \mathbf{H} \tag{6}$$

where $\hat{\mathbf{g}}$ is the spectroscopic splitting tensor. Using a perturbative approach it is possible to show that, under opportune hypothesis, the components of $\hat{\mathbf{g}}$ are given by[49]

$$\hat{\mathbf{g}} = g_e \mathbf{1} + 2\lambda \hat{\Lambda} \tag{7}$$

with

$$\hat{\Lambda} = \begin{bmatrix} \Lambda_{xx} & \Lambda_{xy} & \Lambda_{xz} \\ \Lambda_{yx} & \Lambda_{yy} & \Lambda_{yz} \\ \Lambda_{zx} & \Lambda_{zy} & \Lambda_{zz} \end{bmatrix} = \sum_{n \neq G} \frac{\langle G|\mathbf{L}|n\rangle\langle n|\mathbf{L}|G\rangle}{E_n - E_G} \tag{8}$$

where λ is the spin-orbit coupling constant, $\mathbf{L}$ is the angular momentum operator in units of $\hbar$, while $|G\rangle$ and $|n\rangle$ are the ground and the excited states, respectively. Equation (7) points out that the deviations of $\hat{\mathbf{g}}$ from the value for the free electron, g_e, and its matrix nature are due to the term $2\lambda\hat{\Lambda}$. In general, the calculation of the elements Λ_{ij} is not a simple task, mainly because realistic expressions of $|n\rangle$ and $E_n - E_G$ are not known. However, in many cases of interest a large number of properties of the paramagnetic center can be deduced from Eq. (7) and Eq. (8) and applying simple symmetry considerations. For example, if the paramagnetic center consists in an electron in a spherically symmetric orbital, then $\mathbf{L}|G\rangle = 0$ and all the components Λ_{ij} are zero. As a consequence, the matrix $\hat{\mathbf{g}}$ reduces to the scalar quantity g_e and the EPR spectrum consists of a symmetric resonance line. Similar arguments have been used by Vanheusden and Stesmans[43,44] to point out that for the microscopic structure they proposed for the E'_δ center, the anisotropy of the matrix $\hat{\mathbf{g}}$ is expected to be negligible. The same considerations were applied also to the models proposed by Griscom and Friebele[18] and Zhang and Leisure[20] for the E'_δ center, with the only difference that in these cases the four Si sp^3 hybrid orbitals project into the cavity instead of outward from a central atom. At variance, for the microscopic models of the E'_δ center proposed by Tohmon *et al.*[19] (2-Si model) and by Conley and Lenahan[46] (1-Si model) an axial symmetric $\hat{\mathbf{g}}$ matrix is expected, as for the E'_γ center, in disagreements with the near spherically symmetric EPR line shape observed experimentally for the E'_δ center. We would like to stress that, although the above reported considerations cannot be considered conclusive, if properly used, they could give insight on some relevant EPR properties of a paramagnetic center.

2.1.2. *Hyperfine tensor* $\hat{A}$

When an unpaired electron is localized in the vicinity of a nucleus with nuclear spin $I \neq 0$, another term has to be considered in the Hamiltonian of the paramagnetic system. This term describes the interaction of the electron spin magnetic moment with that of the nucleus and can be expressed in the following general form:[49,71,73]

$$\mathcal{H}_{\text{hyperfine}} = A_0\mathbf{S}\cdot\mathbf{I} + \mathbf{S}\cdot\mathbf{T}\cdot\mathbf{I} = \mathbf{S}\cdot\hat{\mathbf{A}}\cdot\mathbf{I} \tag{9}$$

with

$$A_0 = \frac{2\mu_0}{3} g_e \mu_B g_n \mu_n |\Psi(0)|^2 \tag{10}$$

$$\hat{\mathbf{A}} = A_0\mathbf{1} + \mathbf{T} \tag{11}$$

where $\mu_0 = 1.25664 \cdot 10^{-6}$ H/m is the permeability of free space, g_n is the nuclear spectroscopic splitting factor, μ_n is the nuclear magnetic moment and $|\Psi(0)|^2$ is the squared modulus of the electronic wave function calculated at the position of the nucleus. The operators $A_0\mathbf{1}$ and $\mathbf{T}$ describe the *Fermi contact* and the *dipole-dipole* interactions, respectively. The complete Hamiltonian taking into account Zeeman and Hyperfine interactions is:

$$\mathcal{H} = \mu_{\mathrm{B}} \mathbf{S} \cdot \hat{\mathbf{g}} \cdot \mathbf{H} + \mathbf{S} \cdot \hat{\mathbf{A}} \cdot \mathbf{I} \,. \tag{12}$$

In general, the directions of the principal axis of the operators $\hat{\mathbf{g}}$ and $\hat{\mathbf{A}}$ do not coincide, consequently the diagonalization of the Hamiltonian of Eq. (12) is a complex problem.[49,71,73] However, for many paramagnetic systems, as those of interest in the present work, the principal axis of the operators $\hat{\mathbf{g}}$ and $\hat{\mathbf{A}}$ are nearly coincident and the energies values can be easily obtained. The effect of the hyperfine interaction on such a system of paramagnetic centers with $S = 1/2$ and $I = 1/2$ is that the single resonance at $H_r = h\nu/g_e\mu_{\mathrm{B}}$ is replaced by a pair of lines with center of gravity approximately on H_r and split by A_0.[49,71] Note that, since A_0 is proportional to $|\Psi(0)|^2$, also the hyperfine splitting is expected to be proportional to $|\Psi(0)|^2$.

Another important property of these paramagnetic systems is related to the EPR intensity ratio, ζ, between the hyperfine doublet and the main resonance line. The expected value of ζ for an unpaired electron interacting with a nucleus of ^{29}Si is:[18,20]

$$\zeta = \frac{\text{hyperfine doublet EPR intensity}}{\text{main resonance EPR intensity}} \cong 0.047 \cdot n \cdot (1 - 0.047)^{(n-1)} \,, \tag{13}$$

where 0.047 is the natural abundance of ^{29}Si nuclei and n indicates that the unpaired electron wave function is delocalized over n Si atoms. ζ increases on increasing n because the hyperfine intensity is related to the number of equivalent Si sites of the defect in which the ^{29}Si nucleus can be found. Consequently, obtaining an experimental estimation of ζ, the number n of atoms over which the unpaired electron wave function is delocalized can be determined, so gaining information on the microscopic structure of the paramagnetic center.

2.2. *Systems with spin $S = 1$: Triplet state centers*

In this paragraph we consider a paramagnetic system consisting of two electrons located at distances lower than ~ 5 Å. Due to the low distance between the electrons, two other important interactions are effective and have to be considered in the Hamiltonian: the *electron-electron dipole* and the *electron-exchange* interactions. As can be easily shown,[49] the effect of the latter is to couple the electron spins $S_1 = 1/2$ and $S_2 = 1/2$ to give a diamagnetic singlet state with $S_{\mathrm{tot}} = 0$ and a paramagnetic triplet state with $S_{\mathrm{tot}} = 1$. If, for simplicity, we neglect the hyperfine interaction and the anisotropy of $\hat{\mathbf{g}}$ and if we suppose that the wave functions of the electrons are in the form of a product of the orbital and of the spin components,

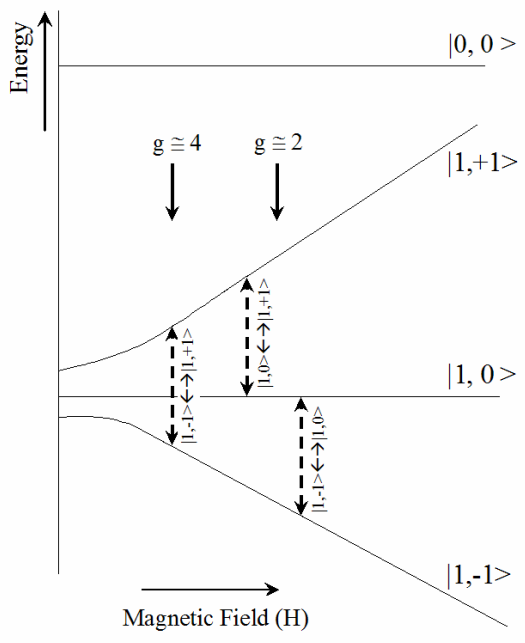

Fig. 1. Schematic representation of the energy levels of a pair of interacting electrons as a function of the modulus of the magnetic field **H**. The transitions observable in an EPR experiment are indicated by broken arrow. In this figure $J_0 < 0$ has been supposed.

then the Hamiltonian of two interacting electrons in the spin triplet state can be written as follow:[49]

$$\mathcal{H} = \mu_B g \mathbf{H} \cdot \mathbf{S}_{tot} + \mathbf{S}_{tot} \cdot \mathbf{D}_{dip} \mathbf{S}_{tot} + J_0 \left(\frac{1}{2} \mathbf{S}_{tot}^2 - \frac{3}{4} \mathbf{1} \right) \tag{14}$$

with

$$\mathbf{D}_{dip} = \frac{\mu_0}{8\pi} (g\mu_B)^2 \begin{bmatrix} \left\langle \frac{r^2 - 3x^2}{r^5} \right\rangle & \left\langle \frac{-3xy}{r^5} \right\rangle & \left\langle \frac{-3xz}{r^5} \right\rangle \\ \left\langle \frac{-3xy}{r^5} \right\rangle & \left\langle \frac{r^2 - 3y^2}{r^5} \right\rangle & \left\langle \frac{-3yz}{r^5} \right\rangle \\ \left\langle \frac{-3xz}{r^5} \right\rangle & \left\langle \frac{-3yz}{r^5} \right\rangle & \left\langle \frac{r^2 - 3z^2}{r^5} \right\rangle \end{bmatrix} \tag{15}$$

$$J_0 = -2 \left\langle \phi_a(1)\phi_b(2) \left| \frac{e^2}{4\pi\varepsilon_0 r} \right| \phi_a(2)\phi_b(1) \right\rangle \tag{16}$$

where $\mathbf{S}_{tot} = \mathbf{S}_1 + \mathbf{S}_2$ is the total spin operator obtained summing over the spins angular momenta of the two electrons $\mathbf{S}_1$ and $\mathbf{S}_2$, ϕ_a and ϕ_b are the spatial parts of the wave functions of the two electrons. The term in Eq. (14) containing the operator $\mathbf{D}_{dip}$ describe the electron-electron dipole interaction, while the term with J_0 is

the electron-exchange interaction. The constant J_0 is known as isotropic electron-exchange coupling constant.[49] Choosing as basis set the eigenstates of the operator $\mathbf{S}_{\text{tot}}$ and of its projection on the direction of $\mathbf{H}$, indicated as $|\mathbf{S}_{\text{tot}}, M\rangle$, the energies of the system of coupled electrons are:[49]

$$E(\mathbf{S}_{\text{tot}} = 0) = -\frac{3}{4}J_0 \tag{17}$$

$$E_{X,Y}(\mathbf{S}_{\text{tot}} = 1) = \frac{1}{4}J_0 + \frac{1}{2}\{D_Z \pm [4g^2\mu_{\text{B}}^2 H^2 + (D_X - D_Y)^2]^{1/2}\} \tag{18}$$

$$E_Z(\mathbf{S}_{\text{tot}} = 1) = \frac{1}{4}J_0 - D_Z \tag{19}$$

where X, Y and Z are the principal axis of the projection of the operator $\mathbf{D}_{\text{dip}}$ in the subspace of states with $\mathbf{S}_{\text{tot}} = 1$ and D_X, D_Y and D_Z are its diagonal values, whereas H is the modulus of the magnetic field $\mathbf{H}$ supposed directed along Z. From Eq. (14) and Eqs. (17)–(19) the following properties of the system of two interacting electrons can be outlined (see Fig. 1):[49]

(i) The exchange interaction separates the energies of the singlet ($\mathbf{S}_{\text{tot}} = 0$) with respect to those of the triplet states ($\mathbf{S}_{\text{tot}} = 1$). Furthermore, if $J_0 < 0$ and $|J_0| \gg k_b T$, where k_b is the Boltzmann constant and T is the temperature, only the paramagnetic triplet state is populated. Conversely, if $J_0 \gg k_b T$ only the diamagnetic singlet state is populated.

(ii) The states $|1, +1\rangle$, $|1, 0\rangle$ and $|1, -1\rangle$ are eigenstates of the Hamiltonian only for a magnetic field $\mathbf{H}$ large enough that the Zeeman interaction dominates on the dipolar term.

(iii) Since, in general, the three triplet eigenstates of the system are linear combinations of pure $|m_s = -1\rangle$, $|m_s = 0\rangle$, $|m_s = +1\rangle$ states, the selection rule $\Delta M = \pm 1$ does not apply. Consequently, together with the allowed transitions $|1, -1\rangle \leftrightarrow |1, 0\rangle$ and $|1, 0\rangle \leftrightarrow |1, +1\rangle$ giving rise to a pair of lines with center of gravity at $g \cong 2$, the transition between the lowest and the highest energy levels of the triplet can be observed, giving an EPR line at $g \cong 4$.

(iv) In general, due to the dipolar interaction, the energies of the levels are not linear functions of the amplitude of the field $\mathbf{H}$.

(v) The three states of the system are not degenerate for $H = 0$, the energy differences depending on the relative orientations of the field $\mathbf{H}$ with respect to the principal axis of the operator $\mathbf{D}_{\text{dip}}$.

3. Experimental Procedures

All the materials considered here are commercial a-SiO_2. Two of these are obtained from fused quartz, QC and Pursil 453,[74] while a third material, KUVI,[75] is synthesized by vapor axial deposition technique. The optical absorption spectra of these materials show an intense band peaked at $\sim$7.6 eV of amplitude of $\sim$20 cm^{-1} for KUVI, and larger than 100 cm^{-1} for Pursil 453 and QC, characterizing them

as oxygen deficient silicon dioxide.[76] Furthermore, all these materials have an Al atoms content of about 10^{17} cm^{-3}.[74,75] γ-ray irradiation has been carried out at room temperature and with dose rate ~ 7 kGy/h. Different samples of Pursil 453 were irradiated in the dose range from 5 kGy to 10^4 kGy. Successively, a sample of this material irradiated at a dose of $\sim 10^3$ kGy was subjected to isochronal thermal treatments from 330 K to 800 K with temperature step of 10 K. Two samples of the KUVI material, hereafter referred to as KUVI/1 and KUVI/2, were simultaneously irradiated at a dose of ~ 124 kGy and were successively subjected to a series of isothermal treatments at fixed temperatures of 580 K and 630 K, respectively. A sample of QC, irradiated at ~ 73 kGy, was isothermally treated at 630 K. In all the thermal treatment experiments the sample was kept at a fixed temperature for a time t_0 and then was cooled to room temperature to perform the EPR measurements. For isochronal treatments t_0 was fixed at 25 minutes whereas for isothermal treatments t_0 was varied from 30 seconds up to many minutes with a sequence depending on the experiment. Finally, to study the microwave saturation properties of the hyperfine doublet of the E'_γ center split by ~ 42 mT, a sample of fused quartz EQ906,[74] γ-ray irradiated at a dose of $\sim 10^3$ kGy, was also considered. In this material no absorption band peaked at ~ 7.6 eV was detected. The typical dimensions of the samples considered in the present work are $5 \times 5 \times 1$ mm^3.

EPR measurements were carried out at room temperature with a Bruker EMX spectrometer working at frequency $\nu \approx 9.8$ GHz (X-band) and with magnetic-field modulation frequency of 100 kHz. EPR spectra have been acquired in the first-harmonic unsaturated mode (FH-EPR) and in the high-power second-harmonic mode (SH-EPR). The latter measurements were used to reveal the 10 mT hyperfine doublet when a large sensitivity was required. Concentration of defects was determined, with relative accuracy of 10%, by double integration of the FH-EPR spectra and by comparison with the double integral of E'_γ center in a reference sample. The defects concentration in the latter was evaluated, with absolute accuracy of 20%, using the instantaneous diffusion method in spin-echo decay measurements carried out in a pulsed EPR spectrometer.[77]

4. Results and Discussion

4.1. *γ-ray irradiation induced point defects*

4.1.1. *E'_γ and E'_δ centers*

In all the samples no EPR signal was detected before irradiation. At variance, after irradiation many distinct EPR signals are induced. In Fig. 2(a) the spectrum centered in correspondence to $g \sim 2$ and obtained for a sample of Pursil 453 irradiated at 10^3 kGy (continuous line) is reported. This EPR signal arises from the partial superposition of two distinct resonance lines ascribed to E'_γ and E'_δ centers.[18] These two contributions were separated by fitting the spectrum with a weighted sum of an experimental line shape for E'_γ center [Fig. 2(c)],[78] and a simulated line shape

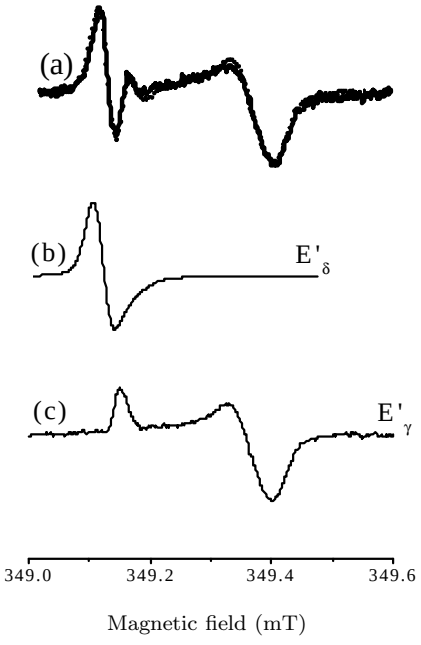

Fig. 2. (a) FH-EPR spectrum for the sample of Pursil 453 irradiated at 10^3 kGy acquired in correspondence of $g \sim 2$ (continuous line) compared to the line obtained as a weighted sum (circles) of the reference lines for (b) E'_δ and (c) E'_γ centers. After Ref. 24.

for E'_δ center [Fig. 2(b)]. The latter was obtained by the Bruker's SimFonia software. The result of this procedure is reported in Fig. 2(a), where the weighted sum (circles) of the reference line shapes for E'_γ and E'_δ is superimposed to the experimental spectrum (continuous line). From the analysis reported in Fig. 2, and fixing $g_\parallel = 2.0018$ for E'_γ,[1] a zero crossing g value of 2.0020 ± 0.0001 has been obtained for E'_δ center, in good agreement with other experimental estimations.[18,27,28,33,42–45] Spectra similar to the one reported in Fig. 2(a) have been observed in all the irradiated oxygen deficient materials considered, whereas in the EQ906 material only the E'_γ resonance is induced.

The line shapes reported in Figs. 2(b) and 2(c) were also used to estimate the concentrations of E'_γ and E'_δ induced in other samples of Pursil 453 irradiated to different γ-ray doses. The growth kinetics of the defects as a function of the γ-ray dose is reported in Fig. 3. The concentration of E'_δ centers was found to increase with irradiation dose up to $\sim 10^2$ kGy. For higher doses a maximum concentration of $\sim 10^{16}$ spins/cm^3 is maintained, suggesting a generation process from precursor defects. At variance, the concentration of E'_δ centers increases up to the highest dose considered, indicating a more complex generation process that could involve a direct activation of normal matrix sites or a not complete exhaustion of precursor defects. Similar concentration growths were previously reported for an X-ray irradiated synthetic a-SiO_2 material.[20]

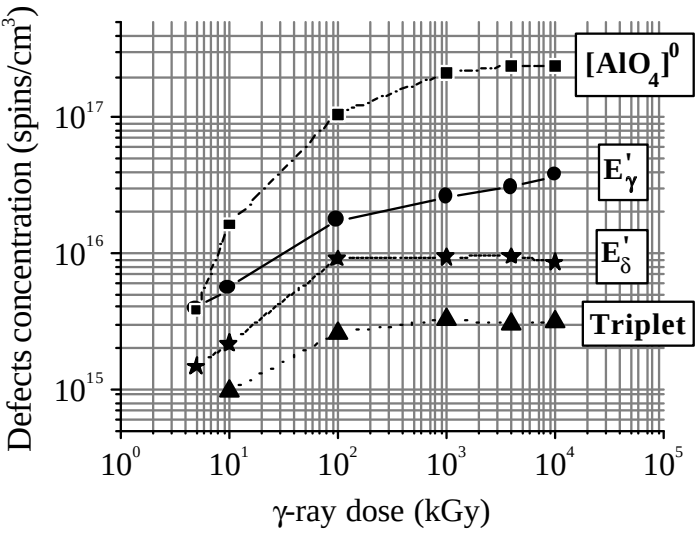

Fig. 3. Concentration of γ-ray irradiation induced paramagnetic defects in Pursil 453. After Ref. 24.

The hyperfine doublets split by 42 mT and 10 mT, associated to E'_γ and E'_δ centers respectively, were also investigated by EPR measurements in the oxygen deficient samples. However, due to the low concentration of defects, a quantitative analysis was prevented.

4.1.2. $[AlO_4]^0$ *center*

After γ-ray irradiation another paramagnetic center was also induced in the oxygen deficient samples. The value of the resonant magnetic field and the characteristics of the FH-EPR line shape, have permitted us to associate this resonance to the $[AlO_4]^0$ center.[79,80] Experimental[81–83] and theoretical[84,85] studies in quartz have shown that this defect consists in a Al atom substituting for a four-coordinated Si atom in the lattice with a hole trapped in a nonbonding 2p orbital of an O atom adjacent to Al. The existence of the analogous defect in a-SiO_2 was also verified.[79,80] In Fig. 3 the growth of concentration of this impurity center on increasing irradiation dose in the material Pursil 453 is reported. As shown in the figure, the $[AlO_4]^0$ center concentration was found to increase up to $\sim 10^3$ kGy and, for higher doses, a limit value of $\sim 2 \times 10^{17}$ spins/cm^3 is maintained. Since this concentration of defects is comparable with the nominal Al content of the material, we conclude that almost all the Al atoms in the material are substitutional of Si and, after irradiation, give rise to the $[AlO_4]^0$ center.

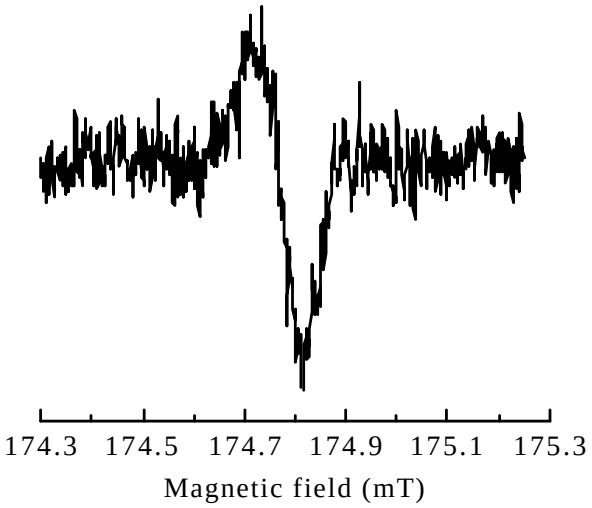

Fig. 4. FH-EPR spectrum for the sample of Pursil 453 irradiated at 10^4 kGy acquired in correspondence of $g \sim 4$. After Ref. 24.

4.1.3. *Triplet center*

In the irradiated oxygen deficient samples we looked for the $g \sim 4$ resonance of the triplet center. To this aim we have performed measurements setting the magnetic field at approximately half of the resonance field of the E' centers. As reported in Fig. 4 for the sample of Pursil 453 irradiated at 10^4 kGy, a FH-EPR signal was detected with line shape and resonance magnetic field compatible with those ascribed to the triplet center.[18,19]

To obtain an estimation of the triplet centers concentration, the intensity of the FH-EPR lines split by ~ 13 mT due to the allowed transitions between the states $|m_s = -1\rangle \leftrightarrow |m_s = 0\rangle$ and $|m_s = 0\rangle \leftrightarrow |m_s = +1\rangle$ had to be determined.[18] In our samples, due to the presence of the intense EPR signal of the $[AlO_4]^0$ centers, we were not able to isolate these lines. However, since it was reported for the triplet center in a-SiO_2 that the ~ 13 mT pair is ~ 2500 times more intense than the $g \sim 4$ resonance,[18] we have roughly estimated the concentration of triplet centers multiplying by a factor 2500 the double integral of the $g \sim 4$ FH-EPR signal. The values obtained for various irradiation doses are reported in Fig. 3. From the comparison of the growth characteristics of E'_δ and triplet centers, it is evident that the maximum value of concentration is reached at the same dose. The concomitant presence of E'_δ and triplet centers in our material, together with the analogy in the growth of concentration with irradiation dose, indicates the existence of some correlation between these two centers. In particular, these features are compatible with the hypothesis that these two centers could arise from the same precursor.[18–20]

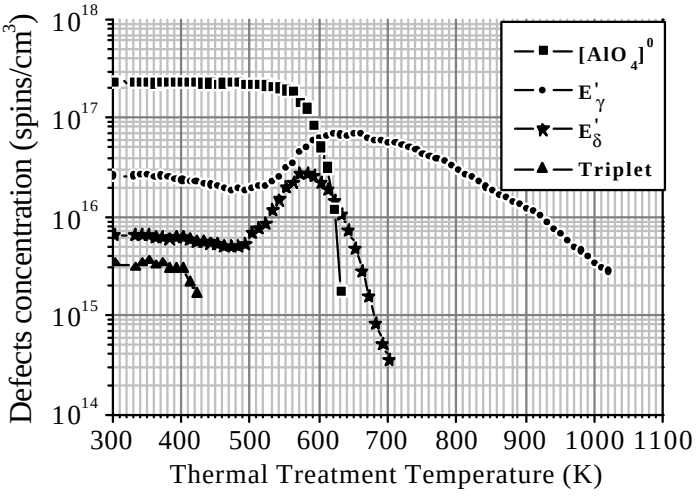

Fig. 5. Concentrations of the paramagnetic defects in the sample of Pursil 453 irradiated at 10^3 kGy as a function of the temperature of the isochronal thermal treatment. After Ref. 24.

4.2. *Effects of thermal treatments*

A sample of Pursil 453 irradiated at 10^3 kGy was subjected to isochronal thermal treatments. The concentrations of defects as a function of the treatment temperatures are reported in Fig. 5. These data show that E'_γ, E'_δ and triplet centers start to anneal at $T \sim 400$ K. However, while at higher temperature the triplet center anneals out definitively, the E'_γ and E'_δ centers concentrations begin to increase for $T \cong 500$ K, indicating that a production mechanism is activated. Maximum concentrations $\sim$3–4 times larger than the initial values are reached after treatments at $T \sim 580$ K and $T \sim 620$ K for E'_δ and E'_γ, respectively. For higher temperature E'_δ and E'_γ centers anneal definitively.

Quite different annealing features were found for $[AlO_4]^0$ centers. As shown in Fig. 5, thermal treatments up to $T \sim 500$ K do not significantly change the concentration of these defects, while for higher temperature the number of defects decreases, undergoing a more rapid annealing with respect to that of E' centers. In particular, $[AlO_4]^0$ centers anneal out in the same temperature range in which the growth of E'_δ and E'_γ centers occurs and, after each thermal treatment, the total number of the generated E' centers is less than that of annealed $[AlO_4]^0$ centers. A similar temperature dependence, occurring in the same temperature range, is typically observed in quartz.[14] In that case, by a detailed EPR analysis, a hole transfer process from $[AlO_4]^0$ to the precursors of E'_1 center was supposed.[14] The analogies between the annealing features observed in our samples with that reported for quartz, suggest that a similar process could occur in a-SiO_2 materials. Furthermore, the generation of E' centers by a hole transfer process indicates that the defects induced in our bulk sample are positively charged, as previously pointed

out for film samples.[42,27,28] In this respect the thermally induced E'_γ center could be considered the direct analogous in a-SiO_2 of the E'_1 center of quartz. In more details, the E'_γ center induced during annealing should originate from an oxygen vacancy that, by trapping an hole, becomes paramagnetic, as well as the E'_1.

The annealing curves of E'_δ and E'_γ centers during the isochronal thermal treatment experiment (Fig. 5) show that the concentration of the former increases up to $T \sim 580$ K whereas that of the latter up to $T \sim 620$ K. Furthermore, for higher temperatures the rate of annealing is different for the two defects. These features should be considered as strong suggestion of different precursors for these defects. In fact, if an oxygen vacancy were a precursor for both E'_δ and E'_γ, there should be no reason to observe temperature differences in their increase, since the common generation process of hole trapping. Also, if these two defects consist in a ionized oxygen vacancy then a similar annealing rate is expected, in contrast with our finding. On these bases it can be guessed that the single oxygen vacancy, precursor of the E'_γ, is not a reliable precursor for the E'_δ center.

We have verified that an increase of E'_γ and E'_δ centers' EPR signals similar to that discussed above for the Pursil 453 occurs also in the samples KUVI/1, KUVI/2 and QC, isothermally treated at 580 K, 630 K and 630 K, respectively. In particular, we have found that the concentration of E'_δ centers grows up to a total time of the isothermal treatment of ~ 500 seconds, after that the defects progressively anneal out.

4.3. *Correlation between the E'_δ center and the 10 mT doublet*

In the sample Pursil 453, for temperature of the treatment in the range from 450 K to 650 K, the 10 mT doublet can be isolated in the second harmonic spectra, as shown in Fig. 6(a) for $T \sim 580$ K. The 7.4 mT doublet characteristic of a hydrogenated point defect is also distinguishable in this spectrum.[56] Similarly, the 10 mT doublet has also been observed in the samples KUVI/1, KUVI/2 and QC for times of isothermal treatments higher than ~ 10 seconds. To support the attribution of the 10 mT doublet to the hyperfine structure of the E'_δ center, we have performed a comparative study of the E'_δ center and of the 10 mT doublet EPR signals in all these samples. The EPR signals intensities of the E'_δ and of the 10 mT doublet were estimated by the fit procedures described in Fig. 2 and in Fig. 6(b), respectively. The latter figure points out that the right component of the 10 mT doublet can be properly fitted by a superposition of three Gaussian profiles: one describes the tail on the left side of the spectrum, while the other two Gaussians take into account the right components of the 7.4 mT and of the 10 mT doublets. The SH-EPR intensity of the right component of the 10 mT doublet was obtained by simple integration of the Gaussian profile peaked at ~ 354 mT. With a similar procedure the SH-EPR signal intensity of the left component of the 10 mT doublet was also estimated, and the total intensity was obtained by summing the contributions of the two components. We note that, to avoid a possible contribution under the 10 mT doublet coming

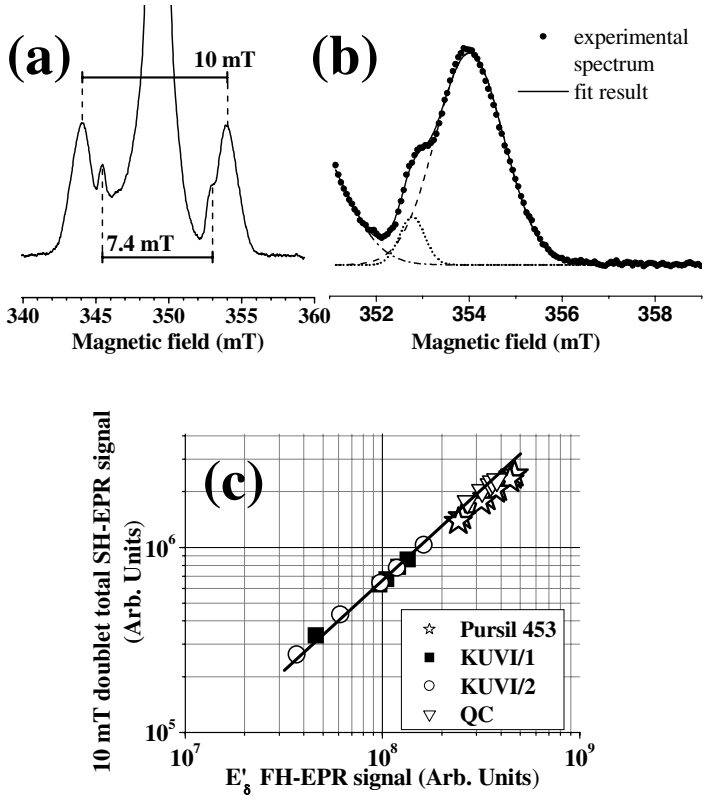

Fig. 6. (a) High-power second-harmonic EPR spectrum of the 10 mT doublet and (b) of its right component detected by SH-EPR measurements for a sample of Pursil 453 irradiated at $\sim 10^3$ kGy and subjected to isochronal thermal treatments up to ~ 580 K. In (b) broken lines indicate the three Gaussians components used to fit the experimental data. (c) SH-EPR total intensity of the 10 mT doublet as a function of the FH-EPR signal intensity of the E'_δ center main resonance for the thermally treated samples. The dimension of the symbols are comparable with the error on the measurements. The straight line, with slope 1, is superimposed to the data, for comparison. After Ref. 24.

from the $|m_s = -1\rangle \leftrightarrow |m_s = 0\rangle$ and $|m_s = 0\rangle \leftrightarrow |m_s = +1\rangle$ triplet transitions, before acquiring the hyperfine doublet we verified that the $g \sim 4$ resonance was absent,[18,20] ensuring that the thermal treatments annealed the triplet center.

In Fig. 6(c) we report the SH-EPR signal of the 10 mT doublet in the samples Pursil 453, KUVI/1, KUVI/2 and QC as a function of the E'_δ center main line FH-EPR signal, as estimated during the thermal treatments experiments. In the figure, the two EPR signals show a strict correlation for an overall variation of their amplitudes of more than one order of magnitude. This result strongly supports the attribution of the 10 mT doublet to the hyperfine structure of the E'_δ center, arising from the hyperfine interaction of the unpaired electron with a nucleus of ^{29}Si ($I = 1/2$).

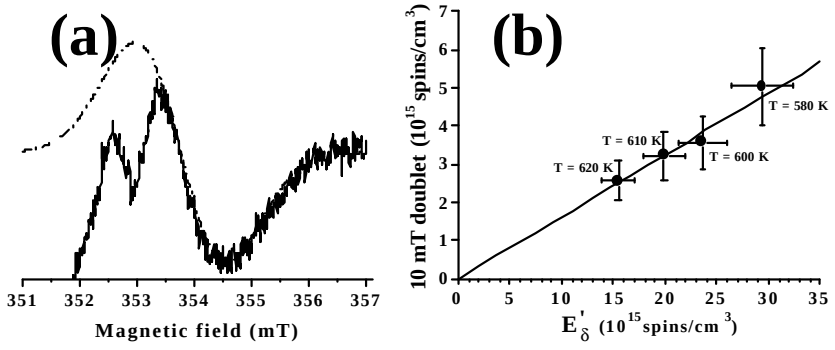

Fig. 7. Pursil 453 sample irradiated at a γ-ray dose of $\sim 10^3$ kGy: (a) First-harmonic unsaturated EPR spectrum (noisy line), after the thermal treatment at ~ 580 K. Superimposed to the spectrum is a derivative Gaussian line shape (broken line). (b) Concentration of defects responsible for the 10 mT doublet as a function of E'_δ concentration during the isochronal thermal treatment experiment. After Ref. 22.

4.4. *Estimation of the intensity ratio between the 10 mT doublet and the E'_δ center main line*

To obtain an experimental estimation of the ratio ζ for the E'_δ center, FH-EPR spectra were also performed for the 10 mT doublet in the Pursil 453 sample after thermal treatments that maximizes the signal. In Fig. 7(a) (noisy line) the spectrum for the right component of the doublet is reported for $T \sim 580$ K. We note that partially superimposed to the signal of the 10 mT line, on the low field side of the spectrum, are some structures that vanish for magnetic field higher than ~ 353.5 mT. Since from SH-EPR measurements we verified that each line of the 10 mT doublet is well described by a Gaussian profile [see Fig. 6(b)], to evaluate the intensity of the 10 mT signal we have superimposed a Gaussian derivative line to the experimental spectrum [broken line in Fig. 7(a)]. From this intensity the concentration of centers responsible for the 10 mT doublet was determined. This analysis was also repeated after isochronal thermal treatments at $T = 600$ K, $T = 610$ K and $T = 620$ K and the obtained concentrations are reported in Fig. 7(b) as a function of E'_δ center concentrations. These data points show a linear correlation, the slope being the ratio ζ. Performing a best fit procedure the value $\zeta = 0.16 \pm 0.02$ was obtained. This intensity ratio is consistent with the value $\zeta = 0.163$ expected for $n = 4$ [see Eq. (13)], indicating that the unpaired electron wave function of the E'_δ center is actually delocalized over four nearly equivalent silicon atoms.

4.5. *Saturation with microwave power of the EPR signals*

To better characterize E'_γ and E'_δ defects, the room temperature saturation properties of their FH-EPR signals with microwave power were studied. These data are reported in Fig. 8(a) for the sample Pursil 453 irradiated at 10^4 kGy and point out

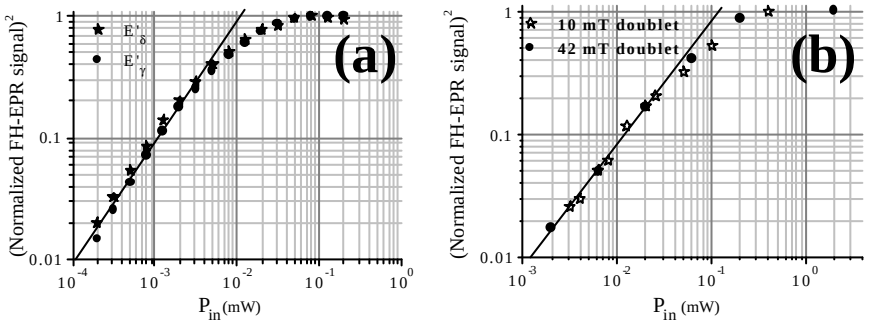

Fig. 8. (a) Room temperature saturation with microwave power of the FH-EPR signal for E'_γ (circles) and E'_δ (stars) centers induced in the sample of Pursil 453 irradiated at 10^4 kGy. (b) Room temperature saturation with microwave power of the FH-EPR signal of the 10 mT doublet in the sample of Pursil 453 irradiated at 10^3 kGy thermally treated at $\sim$580 K (stars) and of the 42 mT doublet in the sample of EQ906 irradiated at 10^3 kGy (circles). Solid lines evidence the linear region of signal growth with microwave power. After Ref. 24.

that the two E' centers have virtually identical saturation properties. Moreover, these saturation curves also reproduce those reported for Type I-IV commercial a-SiO_2.[18,86]

For sake of comparison, the 10 mT and the 42 mT doublets, hyperfine structure of E'_δ and E'_γ centers, respectively, has been also investigated in the same sample. The dependence of the FH-EPR intensity of the 10 mT doublet on microwave power has been obtained taking advantage of the high signal to noise ratio reached during the isochronal thermal treatment experiment and is reported in Fig. 8(b) for the sample treated at 580 K. At variance, due to the superposition with other EPR signals, a reliable saturation curve with microwave power for the 42 mT doublet was not obtained in the same sample. For this reason, we have considered an irradiated sample of EQ906 in which a concentration of $\sim 10^{17}$ spins/cm^3 of E'_γ (and no E'_δ and triplet centers) have been detected. In this sample no spurious signals overlap to the 42 mT doublet, so its room temperature saturation curve with microwave power was obtained and is reported in Fig. 8(b). The comparison proposed in this figure points out that, not only the saturation properties of E'_γ and E'_δ centers are similar, but also those of their hyperfine structures. These strict analogies suggest that the unpaired electron of E'_δ has similar relaxation properties as the E'_γ and that analogous sp^3 orbitals could be involved in both defects.

The dependence of the FH-EPR signal on the microwave power for the $g \sim 4$ resonance was also studied. This EPR signal was found to grow *linearly* with the microwave power up to $\sim$50 mW, whereas deviation from the linear dependence was observed for higher power due to the occurrence of saturation effects. These data point out that saturation of the $g \sim 4$ line occurs at higher power with respect to E'_γ and E'_δ, indicating that the triplet center possesses more effective relaxation channels with respect to the E' centers.

5. Criticism on the Proposed Microscopic Models for the E'_δ Center

Our experimental determination of the intensity ratio between the hyperfine doublet and the main resonance line of the E'_δ center, ζ, has permitted us to point out that the unpaired electron wave function of this center is delocalized over four nearly equivalent silicon atoms. This result definitively rules out that the E'_δ center could consist in a ionized single oxygen vacancy (2-Si model)[19,57–70] or in a defect strongly localized on a single Si atom (1-Si model).[46] In fact, the expected values of ζ for these structures are 0.90 and 0.047, respectively, in disagreement with the value $\zeta = 0.16 \pm 0.02$ we estimated.

In the model of Vanheusden and Stesmans[43,44] the unpaired electron was supposed to possess a wave function resulting from the superposition of four sp^3 orbitals of the silicon atom disposed at the center of the cluster. However, this model leads to a value of $\zeta \cong 0.047$,[20] in disagreement with our estimation.[22] At variance, if one assumes a complementary view in which the unpaired electron is supposed to be delocalized over the outermost four Si atoms of the 5-Si cluster, the unpaired electron should be visualized at any given time as localized in an sp^3 hybrid orbital similar to the one involved in the E'_γ center. The overall orbital should consist in a wave function composed by the four sp^3 orbitals of the nearby Si atoms. This picture is compatible with the analogy found in the continuous-wave microwave saturation properties of E'_δ and E'_γ reported here and with the expected value of ζ. It is worth to note that the conjecture that E'_δ and E'_γ possess similar sp^3 orbitals also agrees with the observed splitting of the hyperfine doublet associated to the E'_δ center. In fact, under this hypothesis, the squared modulus of the electronic wave function at the position of each of the four Si atoms is expected to be one fourth with respect to that of the E'_γ center, due to the delocalization of the unpaired electron. Consequently (see Sec. 2.1.2), the expected splitting of the hyperfine doublet of the E'_δ center is $1/4 \cdot 42$ mT $\cong 10$ mT. The alternative microscopic structure in agreement with our experimental findings is that proposed by Zhang and Leisure (4-Si model).[20] Also in this model, in fact, the unpaired electron is supposed to be delocalized over four sp^3 orbitals of the nearby Si atoms.[20]

Summarizing, our experimental data suggest that the E'_δ center could originate from a radiation induced ionization of an $[SiO_4]$ vacancy [Fig. 9(a)][20] or of a 5-Si cluster [Fig. 9(d)].[43,44] Irradiation removes an electron from one of the Si-Si bonds of the precursor and after a dynamical relaxation the remaining unpaired electron becomes delocalized over four sp^3 hybrid orbitals of the nearby silicon atoms [Fig. 9(b) and Fig. 9(e)].

In our samples a new evidence of the concomitant production and of the similar concentration growth for E'_δ and triplet centers has been found, indicating a correlation between these point defects. If, as already suggested,[18–20] a similar precursor is supposed to be responsible for the generation of E'_δ and triplet centers, then the latter defect could consist in two weakly interacting unpaired electrons localized in

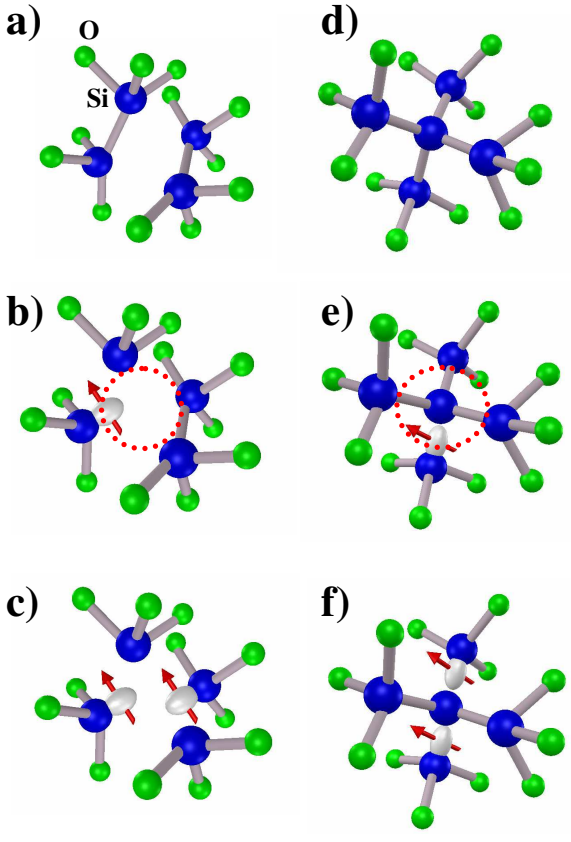

Fig. 9. 4-Si model for the site precursor of (a) E'_δ and triplet centers, (b) E'_δ center and (c) triplet center. 5-Si model for the site precursor of (d) E'_δ and triplet centers, (e) E'_δ center and (f) triplet center. Arrows represent unpaired electrons in Si sp^3 orbitals. After Ref. 24.

two different Si sp^3 orbitals within an $[SiO_4]$ vacancy [Fig. 9(c)] or a 5-Si cluster [Fig. 9(f)]. In this scheme, a single and a double ionization of the same precursor site could be the processes responsible for the generation of the E'_δ and the triplet center, respectively.

6. Conclusions

In conclusion, our data support a structure of E'_δ center in which the unpaired electron is delocalized over four sp^3 hybrid orbitals of nearby Si atoms. This structure agrees with the main experimental evidences of this defect as described in the following: the g tensor is nearly isotropic, as expected for delocalized highly symmetric electronic wave function; the hyperfine splitting of the E'_δ center is ~ 4 times smaller than that of E'_δ center (10 mT $\approx 1/4 \cdot 42$ mT) due to delocalization of the electron over four orbitals similar to the one of E'_γ center; and finally, the

intensity ratio ζ between the 10 mT hyperfine doublet and the E'_δ main EPR line is $\zeta \sim 0.16$, as a consequence of the existence of four nearly equivalent sites of the defect in which the ^{29}Si can be localized.

Acknowledgments

We thank R. Boscaino, M. Cannas, M. Leone, and F. Messina for useful discussions and suggestions, E. Calderaro and A. Parlato for taking care of the γ irradiation in the irradiator IGS-3 at the Nuclear Department of Engineering, University of Palermo. This work was financially supported by Ministry of University Research and Technology.

References

1. *Defects in SiO_2 and Related Dielectrics: Science and Technology*, eds. G. Pacchioni, L. Skuja and D. L. Griscom (Kluwer Academic, Dordrecht, 2000).
2. *Structure and Imperfections in Amorphous and Crystalline Silicon Dioxide*, eds. R. A. B. Devine, J. P. Duraud and E. Dooryhée (Wiley, New York, 2000).
3. D. L. Griscom, D. B. Brown and N. S. Saks, in *The Physics and Chemistry of SiO_2 and Si-SiO_2 Interface*, eds. C. R. Helms and B. E. Deal (Plenum, New York, 1988).
4. F. B. McLean, H. E. Boesch Jr. and T. R. Oldham, in *Ionizing Radiation Effects in MOS Devices and Circuits*, eds. T. P. Ma and P. V. Dressendorfer (Wiley, New York, 1989).
5. R. A. B. Devine, *IEEE Trans. Nucl. Sci.* **41** (1994) 452.
6. E. H. Poindexter and W. L. Warren, *J. Electrochem. Soc.* **142** (1995) 2508.
7. P. M. Lenahan and J. F. Conley Jr., *J. Vac. Sci. Tech.* **B16** (1998) 2134.
8. D. L. Griscom, E. J. Friebele and G. H. Sigel Jr., *Sol. State Commun.* **15** (1974) 479.
9. D. L. Griscom, *Phys. Rev. B* **20** (1979) 1823.
10. M. Boero, A. Pasquarello, J. Sarnthein and R. Car, *Phys. Rev. Lett.* **78** (1997) 887.
11. R. A. Weeks and C. M. Nelson, *J. Am. Ceram. Soc.* **43** (1960) 399.
12. R. H. Silsbee, *J. Appl. Phys.* **32** (1961) 1459.
13. K. L. Yip and W. B. Fowler, *Phys. Rev. B* **11** (1975) 2327.
14. M. G. Jani, R. B. Bossoli and L. E. Halliburton, *Phys. Rev. B* **27** (1983) 2285.
15. J. K. Rudra and W. B. Fowler, *Phys. Rev. B* **35** (1987) 8223.
16. D. C. Allan and M. P. Tetter, *J. Am. Ceram. Soc.* **73** (1990) 3247.
17. V. V. Afanas'ev and A. Stesmans, *J. Phys.: Condens. Matter* **12** (2000) 2285.
18. D. L. Griscom and E. J. Friebele, *Phys. Rev. B* **34** (1986) 7524.
19. R. Tohmon, Y. Shimogaichi, Y. Tsuta, S. Munekuni, Y. Ohki, Y. Hama and K. Nagasawa, *Phys. Rev. B* **41** (1990) 7258.
20. L. Zhang and R. G. Leisure, *J. Appl. Phys.* **80** (1996) 3744.
21. H. Nishikawa, E. Watanabe, D. Ito, Y. Sakurai, K. Nagasawa and Y. Ohki, *J. Appl. Phys.* **80** (1996) 3513.
22. G. Buscarino, S. Agnello and F. M. Gelardi, *Phys. Rev. Lett.* **94** (2005) 125501.
23. S. Agnello, G. Buscarino and F. M. Gelardi, *J. Non-Cryst. Solids* **351** (2005) 1787.
24. G. Buscarino, S. Agnello and F. M. Gelardi, *Phys. Rev. B* **73** (2006) 045208.
25. M. E. Zvanut, R. E. Stahlbush and W. E. Carlos, *Appl. Phys. Lett.* **60** (1992) 2989.
26. R. A. B. Devine, D. Mathiot, W. L. Warren, D. M. Fleetwood and B. Aspar, *Appl. Phys. Lett.* **63** (1993) 2926.

27. J. F. Conley, P. M. Lenahan, H. L. Evans, R. K. Lowry and T. J. Morthorst, *J. Appl. Phys.* **76** (1994) 2872.
28. J. F. Conley, P. M. Lenahan, H. L. Evans, R. K. Lowry and T. J. Morthorst, *Appl. Phys. Lett.* **65** (1994) 2281.
29. W. L. Warren, M. R. Shaneyfelt, D. M. Fleetwood, J. R. Schwank, P. S. Winokur and R. A. B. Devine, *IEEE Trans. Nucl. Sci.* **41** (1994) 1817.
30. W. L. Warren, D. M. Fleetwood, M. R. Shaneyfelt, P. S. Winokur and R. A. B. Devine, *Phys. Rev. B* **50** (1994) 14710.
31. W. L. Warren, D. M. Fleetwood, M. R. Shaneyfelt, J. R. Schwank, P. S. Winokur, R. A. B. Devine and D. Mathiot, *Appl. Phys. Lett.* **64** (1994) 3452.
32. M. E. Zvanut, T. L. Chen, R. E. Stahlbush, E. S. Steigerwalt and G. A. Brown, *J. Appl. Phys.* **77** (1995) 4329.
33. R. A. B. Devine, W. L. Warren, J. B. Xu, I. H. Wilson, P. Paillet and J. L. Leray, *J. Appl. Phys.* **77** (1995) 175.
34. A. Stesmans and V. V. Afanas'ev, *Appl. Phys. Lett.* **69** (1996) 2056.
35. M. E. Zvanut and T. Chen, *Appl. Phys. Lett.* **69** (1996) 28.
36. A. Stesmans, B. Nouwen, D. Pierreux and V. V. Afanas'ev, *Appl. Phys. Lett.* **80** (2002) 4753.
37. A. Stesmans, B. Nouwen and V. V. Afanas'ev, *Phys. Rev. B* **66** (2002) 045307.
38. A. Stesmans, R. Devine, A. G. Revesz and H. Hughes, *IEEE Trans. Nucl. Sci.* **37** (1990) 2008.
39. J. F. Conley Jr., P. M. Lenahan and P. Roitman, *Appl. Phys. Lett.* **60** (1992) 2889.
40. J. F. Conley Jr., P. M. Lenahan and P. Roitman, *IEEE Trans. Nucl. Sci.* **39** (1992) 2114.
41. W. L. Warren, M. R. Shaneyfelt, J. R. Schwank, D. M. Fleetwood, P. S. Winokur, R. A. B. Devine, W. P. Maszara and J. B. McKitterick, *IEEE Trans. Nucl. Sci.* **40** (1993) 1755.
42. W. L. Warren, D. M. Fleetwood, M. R. Shaneyfelt, J. R. Schwank, P. S. Winokur and R. A. B. Devine, *Appl. Phys. Lett.* **62** (1993) 3330.
43. K. Vanheusden and A. Stesmans, *J. Appl. Phys.* **74** (1993) 275.
44. K. Vanheusden and A. Stesmans, *Appl. Phys. Lett.* **62** (1993) 2405.
45. A. Stesmans and K. Vanheusden, *J. Appl. Phys.* **76** (1994) 1681.
46. J. F. Conley and P. M. Lenahan, *IEEE Trans. Nucl. Sci.* **42** (1995) 1740.
47. R. A. B. Devine, D. Mathiot, W. L. Warren and B. Aspar, *J. Appl. Phys.* **79** (1996) 2302.
48. R. E. Walkup and S. I. Raider, *Appl. Phys. Lett.* **53** (1988) 888.
49. J. A. Weil, J. R. Bolton and J. E. Wertz, *Electron Paramagnetic Resonance* (Wiley, New York, 1994).
50. G. K. Celler, P. L. F. Hemment, K. W. West and J. M. Gibson, *Appl. Phys. Lett.* **48** (1986) 532.
51. J. Stoemenos, L. Margail, C. Jaussaud, M. Dupuy and M. Bruel, *Appl. Phys. Lett.* **48** (1986) 1470.
52. V. V. Afanas'ev, A. Stesmans and M. E. Twigg, *Phys. Rev. Lett.* **77** (1996) 4206.
53. V. V. Afanas'ev, A. Stesmans, A. G. Revesz and H. L. Hughes, *Appl. Phys. Lett.* **71** (1997) 2106.
54. V. V. Afanas'ev, A. Stesmans, A. G. Revesz and H. L. Hughes, *J. Appl. Phys.* **82** (1997) 2184.
55. V. V. Afanas'ev and A. Stesmans, *Phys. Rev. B* **59** (1999) 2025.
56. T. Tsai and D. L. Griscom, *J. Non-Cryst. Solids* **91** (1987) 170.
57. P. E. Blöchl, *Phys. Rev. B* **62** (2000) 6158.

58. N. Lopez, F. Illas and G. Pacchioni, *J. Phys. Chem. B* **104** (2000) 5471.
59. T. Uchino, M. Takahashi and T. Yoko, *Phys. Rev. Lett.* **86** (2001) 5522.
60. Z.-Y. Lu, C. J. Nichlaw, D. M. Fleetwood, R. D. Schrimpf and S. T. Pantelides, *Phys. Rev. Lett.* **98** (2002) 285505.
61. C. J. Nicklaw, Z.-Y. Lu, D. M. Fleetwood, R. D. Schrimpf and S. T. Pantelides, *IEEE Trans. Nucl. Sci.* **49** (2002) 2667.
62. J. R. Chavez, S. P. Karna, K. Vanheusden, C. P. Brothers, R. D. Pugh, B. K. Singaraju, W. L. Warren and R. A. B. Devine, *IEEE Trans. Nucl. Sci.* **44** (1997) 1799.
63. S. P. Karna, A. C. Pineda, W. M. Shedd and B. K. Singaraju, *Electrochem. Soc. Proc.* **99-3** (1999) 161.
64. S. P. Karna, H. A. Kurtz, A. C. Pineda, W. M. Shedd and R. D. Pugh, Point defects in Si-SiO_2 systems: current understanding, in *Defects in SiO_2 and Related Dielectrics: Science and Technology*, eds. G. Pacchioni, L. Skuja and D. L. Griscom (Kluwer, Dordrecht, 2000), p. 599
65. A. C. Pineda and S. P. Karna, *J. Phys. Chem. A* **104** (2000) 4699.
66. S. P. Karna, A. C. Pineda, R. D. Pugh, W. M. Shed and T. R. Oldham, *IEEE Trans. Nucl. Sci.* **47** (2000) 2316.
67. S. Mukhopadhyay, P. V. Sushko, A. H. Edwards and A. L. Shluger, *J. Non-Cryst. Solids* **345&346** (2004) 703.
68. S. Mukhopadhyay, P. V. Sushko, A. M. Stoneham and A. L. Shluger, *Phys. Rev. B* **70** (2004) 195203.
69. S. Mukhopadhyay, P. V. Sushko, V. A. Mashkov and A. L. Shluger, *J. Phys.: Condens. Matter* **17** (2005) 1311.
70. P. V. Sushko, S. Mukhopadhyay, A. S. Mysovsky, V. B. Sulimov, A. Taga and A. L. Shluger, *J. Phys.: Condens. Matter* **17** (2005) S2115.
71. A. Abragam and B. Bleaney, *Electron Paramagnetic Resonance of Transition Ions* (Clarendon, 1970).
72. C. P. Poole Jr., *Electron Spin Resonance* (Wiley, New York, 1967).
73. M. Cook and C. T. White, *Semicond. Sci. Technol.* **4** (1989) 1012.
74. Quartz and Silice, Nemours, France, catalogue OPT-91-3.
75. Almaz Optics on line catalog.
76. L. Skuja, *J. Non-Cryst. Solids* **239** (1998) 16.
77. S. Agnello, R. Boscaino, M. Cannas and F. M. Gelardi, *Phys. Rev. B* **64** (2001) 174423.
78. S. Agnello, R. Boscaino, G. Buscarino, M. Cannas and F. M. Gelardi, *Phys. Rev. B* **66** (2002) 113201.
79. R. Schnadt and A. Räuber, *Sol. State Comm.* **9** (1971) 159.
80. D. L. Griscom, in *The Physics of SiO_2 and its Interfaces*, ed. S. T. Pantelides (Pergamon, New York, 1978), p. 232R.
81. J. H. E. Griffiths, J. Owen and I. M. Ward, *Nature* (*London*) **173** (1954) 439.
82. M. C. M. O'Brien and M. H. L. Pryce, in *Defects in Crystalline Solids* (The Physical Society, London, 1955), p. 88.
83. R. H. D. Nuttall and J. A. Weil, *Can. J. Phys.* **59** (1981) 1696.
84. G. Pacchioni, F. Frigoli, D. Ricci and J. A. Weil, *Phys. Rev. B* **63** (2000) 054102.
85. J. To, A. A. Sokol, S. A. French, N. Kaltsoyannis and C. R. A. Catlow, *J. Chem. Phys.* **122** (2005) 144704.
86. S. Agnello, R. Boscaino, F. M. Gelardi and B. Boizot, *J. Appl. Phys.* **89** (2001) 6002.